# Optimization of Lignin Removal from Synthesized Wastewater by Iron (III) Trimesate

**Bhuckchanya Pangkumhang[1], Jakkapop Phanthasri[1], Suttikorn Suwannatrai[1], Pummarin Khamdahsag[2,3], Chitsan Lin[4] and Visanu Tanboonchuy[1,5,6*]**

*[1]Department of Environmental Engineering, Faculty of Engineering, Khon Kaen University, Khon Kaen 40002, Thailand*
*[2]Environmental Research Institute, Chulalongkorn University, Bangkok 10330, Thailand*
*[3]Center of Excellence on Hazardous Substance Management (HSM), Chulalongkorn University, Bangkok 10330, Thailand*
*[4]Department of Marine Environmental Engineering, National Kaohsiung University of Science and Technology, Kaohsiung 81157, Taiwan*
*[5]Research Center for Environmental and Hazardous Substance Management (EHSM), Khon Kaen University, Khon Kaen 40002, Thailand*
*[6]Research Program on Development of Appropriate Technologies for Coloring Agent Removal from Textile Dyeing, Pulp & Paper, and Sugar Industries for Sustainable Management, Center of Excellence on Hazardous Substance Management (HSM), Chulalongkorn University, Bangkok 10330, Thailand*

**ARTICLE INFO**

Received: 25 Oct 2018
Received in revised:
9 Jan 2019
Accepted: 31 Jan 2019
Published online:
22 May 2019
DOI: 10.32526/ennrj.17.4.2019.26

**Keywords:**
Lignin/ Coagulation-flocculation process/ Iron (III) trimesate/ Metal-organic framework/ Box-Behnken design

*** Corresponding author:**
E-mail: visanu@kku.ac.th

**ABSTRACT**

Box-Behnken design (BBD) was employed to study an optimal treatment method of synthetic lignin wastewater effluent from pulp and paper wastewater treatment plants using iron (III) trimesate (Fe-BTC) as an alternative coagulant aid. Fe-BTC was prepared by hydrothermal technique using ferric chloride hexahydrate ($FeCl_3 \cdot 6H_2O$) combined with 1,3,5-benzenetricarboxylic acid (trimesic acid, $H_3BTC$) in deionized water and ethanol. X-ray diffractometry and Fourier transform infrared spectroscopy were used to characterize the property of Fe-BTC. Three quadratic models of the four factors including Fe-BTC dosage, pH, initial lignin concentration, and slow mixing time were defined with lignin removal efficiency as a response. Treatment efficiency of lignin removal was 50-80% for experimental data and 60-80% for predicted values. Optimal condition was 1 g/L of Fe-BTC dosage, pH 4, and 50 ppm of initial lignin concentration without slow mixing giving 58.34% lignin removal efficiency. The pH of treated samples was below 3 after all processes. Results showed that Fe-BTC enhanced separation of lignin by coagulation-flocculation. Adsorption-charge neutralization is the main mechanism of this process at acidic pH. Fe-BTC separated the wastewater into three layers with Fe-BTC powder at the bottom, lignin sludge in the middle, and clear supernatant at the top. Lignin sludge can be reused and recycled for use in other applications.

## 1. INTRODUCTION

Effluent wastewater produced by the pulp and paper (P&P) industry has an adverse environmental impact because it generates large volumes of highly toxic substances. Wastewater treatment plants (WWTPs) use physical, chemical, and biological processes to treat organic/inorganic compounds, acidic resins, heavy metals, suspended solids, surfactant/detergent agents and other chemicals (Kamali and Khodaparast, 2015; Lindholm-Lehto et al., 2015). However, treated effluents from WWTPs still contain high color pollution resulting from lignin and lignin derived substances. These pollutants block sunlight transmission into the water which affects photosynthesis and decreases dissolved oxygen. Degradation of lignin by biological treatment is difficult and may cause transformation into toxic substances as wastewater from cooking and bleaching processes contains lignin and chlorine (Ashrafi et al., 2015; Haq et al., 2017). Hence, removal of the lignin fraction is an important issue. Lignin can be recovered and recycled as an adsorbent, flocculating agent and fuel (Naseem et al., 2016; Roopan, 2017).

Generally, P&P wastewater treatment plants include physicochemical and biological processes to remove solids, suspended solids, colloids and dispersions. In a filtration system, membrane fouling

results from lignin (Zahrim et al., 2015). However, the remaining pollutants may require tertiary treatment. Sludge or secondary waste generated via each treatment process is managed by combustion in an incinerator or disposed of as landfill. Therefore, lignin and lignin fractions become unrecyclable waste (Ali and Sreekrishnan, 2001; Kamali and Khodaparast, 2015; Lindholm-Lehto et al., 2015). Typically, a coagulation-flocculation process is employed by wastewater treatment plants to remove pollutants such as organic/inorganic matter, color, and microorganisms because of its simple operation, low cost, and high efficiency which relies on coagulant-flocculant properties for particle destabilization and agglomeration into larger flocs that can be settled by gravity (Sun et al., 2017).

Conventional aluminum-based and iron-based coagulants and organic-based flocculants are commonly employed (Duan and Gregory, 2003; Sillanpää et al., 2018). Moreover, previous studies reported that iron-based treatment removed dissolved organic carbon (DOC) more efficiently than an aluminum-based approach (Zhan et al., 2010). For this reason, several materials have been developed and improved for economical high-performance removal of pollutants (Jiang, 2015; Folens et al., 2017). To treat wastewater from the P&P industry, alum, polyaluminum chloride (PAC), aluminum chloride, starch-g-PDMC, and chitosan, have all been applied (Renault et al., 2009; Lee et al., 2014; Kamali and Khodaparast, 2015; Lindholm-Lehto et al., 2015). However, sludge generated from these processes becomes a secondary waste that requires proper disposal treatment before dumping.

Recently, many new hybrid materials have been developed to enhance coagulation-flocculation processes. Application of these hybrid materials in the wastewater treatment process has greatly reduced operation time for processing large volumes of discharged wastewater (Lee et al., 2012). Iron (III) trimesate (Fe-BTC) is a well-known hybrid material as a metal-organic framework (MOF) used to remove lignin by the coagulation-flocculation method. This material consists of iron ion/clusters and trimesic acid formed by a hydrothermal technique. Many properties of Fe-BTC include high biocompatibility, stability, large surface area, and strong Lewis acid catalytic activity (Dhakshinamoorthy et al., 2012; Zhu et al., 2012).

Response surface methodology (RSM) is a mathematical statistical method used to calculate the desired response to achieve the optimal condition. To design experiments and investigate the influence of factors, Box-Behnken design (BBD) was selected (Archariyapanyakul et al., 2017; Bezerra et al., 2008; Kim, 2016; Daud et al., 2018; Khamdahsag el al., 2017; Kiattisaksiri et al., 2015). BBD has been used for optimization of acid-catalyzed transesterification biodiesel wastewater pre-treatment (Daud et al., 2018), clove oil development based nanoemulsion of olmesartan for transdermal delivery (Aqil et al., 2016), color and chemical oxygen demand (COD) removal optimization from livestock wastewater (Tak et al., 2015), and arsenic removal by aluminum sulfate (Bilici Baskan and Pala, 2010). Therefore, BBD could be used to evaluate the effect of influential factors and determine optimal condition to maximize the response variables. Here, the influential factors of Fe-BTC dosage, pH, initial lignin concentration and slow mixing time were determined, and the efficiency of lignin removal was investigated as the dependent output variable.

## 2. METHODOLOGY

### 2.1 Materials

All chemical reagents used for the preparation of coagulants were analytical grade including ferric chloride hexahydrate ($FeCl_3 \cdot 6H_2O$) (QRëC, New Zealand), trimesic acid ($H_3BTC$) (Sigma Aldrich, Singapore), alkaline lignin (TCI, America), nitric acid ($HNO_3$), sodium hydroxide (NaOH) (RCI Labscan), ethanol ($C_2H_5OH$) (RCI Labscan), deionized (DI) water, and reverse osmosis (RO) water.

Fe-BTC was synthesized by a hydrothermal technique adapted from previous reports (Zhu et al., 2012; Phanthasri et al., 2018). An amount of 1 mmol $FeCl_3$ was dissolved in 25 mL DI water, then 1 mmol of $H_3BTC$ in 25 mL ethanol was added and the mixture was stirred for 30 min. The solution was placed in a Teflon-lined stainless steel autoclave reactor and heated for 48 h in an oven at 100 $^oC$. The solution was then cooled to ambient temperature and separated by centrifuging. The material was dried in a furnace oven at 100 $^oC$ overnight. Orange powder of Fe-BTC was obtained and stored in a desiccator.

### 2.2 Materials characterization

Crystallinity of Fe-BTC was determined using an X-ray diffractometer (XRD) (D8 Discover,

Bruker AXS) with a Cu Kα radiation (λ=0.1514 nm) at 40 mA and 40 kV. The scan range was 5-70° with an increment of 0.02 °/step, and scan speed of 0.1 sec/step at 298 K. Spectra adsorption of Fe-BTC was obtained using a Fourier-transform infrared (FT-IR) spectrometer (8601 PC, Shimadzu), recorded with KBr pellets and then analyzed over a wavenumber range of 4,000 to 450 $cm^{-1}$. Percentage yield was calculated between actual mass value versus theoretical value.

### 2.3 Coagulation-flocculation test

Coagulation-flocculation experiments were performed using a jar test (Phipps and Bird) apparatus equipped with six paddle stirrers at room temperature (25±1 °C). Synthetic lignin wastewater was prepared by dissolving lignin solid in RO water. The pH of wastewater sample was adjusted by adding $HNO_3$ or NaOH. Fe-BTC were mixed in 500 mL of synthetic lignin for 1.50 min at 200 rpm, then settled for 30 min. Supernatants were withdrawn 2 cm under the surface and filtered through 0.45 μm syringe filters (FilTrex, diameter 13 cm). Effects of environmental factors including dosage, pH, initial lignin concentration, and slow mixing time were investigated to determine the optimal condition using statistical design. After settling, the supernatant was withdrawn from the beaker. Lignin residual was quantified by UV absorbance of the sample at λ=280 nm (Andersson et al., 2011), measured with a UV-vis spectrophotometer (DR 6000™, HACH). Lignin removal efficiency was calculated using Equation 1.

$$\text{Lignin Removal Efficiency (\%)} = \frac{L_i - L_f}{L_i} \times 100 \qquad (1)$$

where $L_i$ is the initial absorbance and $L_f$ is the final absorbance.

### 2.4 Experimental design

Box-Behnken design (BBD) (Ferreira et al., 2007; Bezerra et al., 2008) presents a three-level factorial selection which assists in estimating the first and second coefficients of mathematical models. The number of experiments (N) is defined as $N= 2k(k-1)+ C_p$, (where k is the number of factors and $C_p$ is the number of central points). Factor levels adjusted at low, middle, and high for each variable were designated as -, 0, and +, respectively.

BBD was employed to optimize lignin removal efficiency, with variation in Fe-BTC dosage ($X_1$), pH ($X_2$), initial lignin concentration ($X_3$), and slow mixing time ($X_4$). Experimental conditions were designed (Table 1) and data were analyzed by response surface regression (RSREG) using Mimitab16 software to fit the following second order polynomial (Equation 2):

$$Y = \beta_0 + \sum_{i=1}^{k} \beta_i x_i + \sum_{j=1}^{k} \beta_{ii} x_i^2 + \sum_{i=1}^{k} \sum_{j=1}^{k} \beta_{ij} x_i x_j + \varepsilon \qquad (2)$$

where, Y is the response (removal efficiencies, %); $\beta_0$, $\beta_i$ (i=1, 2, 3, 4) and $\beta_{ij}$ (i=1, 2, 3, 4; j=1, 2, 3, 4) are the model coefficients and $X_i$ and $X_j$ are the coded independent variables.

**Table 1.** Coded factor levels for a BBD of a four independence variable

| Run No. | $X_1$ | $X_2$ | $X_3$ | $X_4$ |
|---|---|---|---|---|
| 1 | + | 0 | 0 | - |
| 2 | 0 | - | 0 | + |
| 3 | 0 | + | 0 | - |
| 4 | 0 | 0 | 0 | 0 |
| 5 | - | 0 | + | 0 |
| 6 | + | - | 0 | 0 |
| 7 | 0 | 0 | - | + |
| 8 | 0 | 0 | + | + |
| 9 | - | 0 | 0 | - |
| 10 | + | 0 | + | 0 |
| 11 | - | 0 | 0 | + |
| 12 | - | - | 0 | 0 |
| 13 | 0 | 0 | + | - |
| 14 | + | + | 0 | 0 |
| 15 | 0 | + | + | 0 |
| 16 | 0 | + | 0 | + |
| 17 | + | 0 | - | 0 |
| 18 | 0 | 0 | 0 | 0 |
| 19 | 0 | - | + | 0 |
| 20 | 0 | - | - | 0 |
| 21 | - | + | 0 | 0 |
| 22 | - | 0 | - | 0 |
| 23 | 0 | - | 0 | - |
| 24 | 0 | + | - | 0 |
| 25 | 0 | 0 | - | - |
| 26 | 0 | 0 | 0 | 0 |
| 27 | + | 0 | 0 | + |

To ensure equation model fitting, two experiments were conducted under chosen conditions compared with predicted values from the fitting models (Equations 1 and 2). A p-value (probability) with 95% confidence level was employed to estimate model terms.

## 3. RESULTS AND DISCUSSION

### 3.1 Material characterization

*3.1.1 Crystallinity of Fe-BTC*

The XRD patterns of Fe-BTC revealed poor crystallinity of Fe-BTC (Figure 1). Low-density diffraction peaks indicated semi-amorphous small sized crystals and disarrayed structure (Autie-Castro et al., 2015; Yang et al., 2016). Highest intensity was indicated by 2θ at 10.8° (Yang et al., 2016).

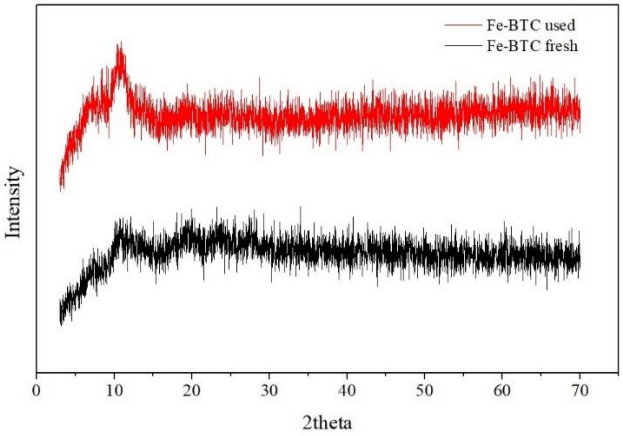


**Figure 1.** X-ray diffraction pattern of Fe-BTC.

*3.1.2 Fourier transform infrared (FT-IR) spectra*

Figure 2 compares FT-IR spectra between fresh and used Fe-BTC. Results found by Hu et al. (2016), Li et al. (2016), Yang et al. (2016), Huang et al. (2017), and Mahmoodi et al. (2018) were comparable to spectra adsorption bands of Fe-BTC found here. Presence of the carboxylate functional group showed infrared absorption bands from 1,300 to 1,700 $cm^{-1}$, and the aromatic benzene ring in bands below 1,300 $cm^{-1}$. Bands from 3,300 to 3,650 $cm^{-1}$ revealed the presence of water molecules. The peak of O-H bond showed at 3,400 and 1,449 $cm^{-1}$; C=O bond at 1,715 and 1,625 $cm^{-1}$; C-O bond at 1,390, 1,220, and 1,050 $cm^{-1}$; C-H bond at 759 and 711 $cm^{-1}$, and Fe-O bond at 484. These results revealed no new peak observations.

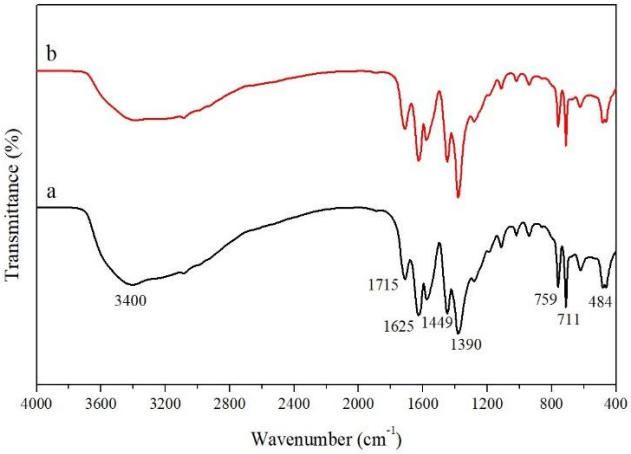


**Figure 2.** FT-IR spectra of Fe-BTC as (a) fresh and (b) used.

*3.1.3 Percentage of Fe-BTC as synthesized*

Fe-BTC was synthesized via the hydrothermal method by $FeCl_3$ combined with $H_3BTC$ as shown in the following chemical reaction,

$$FeCl_3 + H_3BTC \rightarrow \text{Fe-BTC} + 3HCl \quad (4)$$

With balancing, the reaction ratio was 1 mol of $FeCl_3$/1 mol of $H_3BTC$ producing 1 mol of Fe-BTC. Actual mass obtained from the experiment was 0.10-0.12 g and theoretical mass obtained from stoichiometry was 0.26 g, thus %yield of product was 38.46-46.15%.

### 3.2 Statistical analysis

*3.2.1 BBD model fitting*

The experiment was tested under various conditions as follows; Fe-BTC dosage ranged from 1-3 g/L, initial pH ranged from 4-10, initial lignin concentration ranged from 50-150 ppm and slow mixing time at 40 rpm ranged from 0-40 min. Uncoded and coded independent variables and the experimental design matrix obtained from BBD are shown in Table 2 and Table 3, respectively.

**Table 2.** Parameters and levels used in the BBD for lignin removal using Fe-BTC in coagulation-flocculation process.

| Parameters | Symbol | Levels of parameters | | |
|---|---|---|---|---|
| | | -1 | 0 | +1 |
| Fe-BTC dosages (g/L) | $X_1$ | 1.0 | 2.0 | 3.0 |
| pH | $X_2$ | 4.0 | 7.0 | 10.0 |
| Initial lignin concentration (mg/L) | $X_3$ | 50 | 100 | 150 |
| Slow mixing time at 40 rpm (min) | $X_4$ | 0 | 20 | 40 |

Lignin removal and color removal predicted values were obtained by quadratic model fitting techniques (Equation 2) using Mimitab16 software. Equation 4 presents coefficients determined from response plotting as a function of independent variables;

$$Y = 74.2815 - 10.6566X_1 - 1.3909X_2 - 0.0944X_3 + 1.0979X_4 + 5.0638X_1^2 + 0.1927X_2^2 + 0.0021X_3^2 - 0.0257X_4^2 - 0.2594X_1X_2 - 0.1037X_1X_3 - 0.2593X_1X_4 - 0.0105X_2X_3 + 0.0036X_2X_4 + 0.0072X_3X_4 \quad (4)$$

where Y is the percentage of lignin removal, $X_1$ is the quantity of Fe-BTC added (g), $X_2$ is the pH, $X_3$ is the initial concentration of lignin (ppm), and $X_4$ is slow mixing time (min). Coefficients prior to $X_1$, $X_2$, $X_3$ and $X_4$ represent the linear effects of the main factors. Coefficients prior to $X_1X_2$, $X_1X_3$, $X_1X_4$, $X_2X_3$, $X_2X_4$, $X_3X_4$ and $X_1^2$, $X_2^2$, $X_3^2$, $X_4^2$ represent interaction between two factors and the quadratic effects, respectively. A positive sign in front of each term indicates a synergistic effect while a negative sign indicates an antagonistic effect.

In Table 4, normalized standard deviation (S.D.) was applied to compare the most applicable model that could describe the kinetic study of adsorption obtained using the following equation (Luekittisup et al., 2015):

$$\text{S.D.}(\%) = 100 \text{ x } \left\{\sum \frac{[(Y_e - Y_p)/Y_e]^2}{N-1}\right\}^{1/2} \quad (5)$$

where $Y_e$ is the experimental values, $Y_p$ is the predicted values and N is number of data points.

Model predictability achieved greater than 95% confidence level based on initial lignin concentration (p-value=0.049). Results show predicted values obtained from Equation 3. Therefore, the most influential factor affecting lignin removal was initial lignin concentration ($X_3$) as indicated by p-values (Table 3). On the other hand, quantity of Fe-BTC ($X_1$) pH ($X_2$) and slow mixing time ($X_4$) had no significant effect (p-values>0.05).

**Table 3.** Estimated regression coefficients of removal efficiency (%)

| Term | Lignin removal | |
|---|---|---|
| | Coefficient | P value |
| Constant | 74.2815 | 0.000 |
| Dosages (g/L) | -10.6566 | 0.085 |
| pH | -1.3909 | 0.896 |
| [Lignin] (ppm) | -0.0944 | 0.049 |
| Slow mixing time (min) | 1.0979 | 0.181 |
| Dosages (g/L) × Dosages (g/L) | 5.0638 | 0.431 |
| pH × pH | 0.1927 | 0.785 |
| [Lignin] (ppm) × [Lignin] (ppm) | 0.0021 | 0.422 |
| Slow mixing time (min) × Slow mixing time (min) | -0.0257 | 0.125 |
| Dosages (g/L) × pH | -0.2594 | 0.915 |
| Dosages (g/L) × [Lignin] (ppm) | -0.1037 | 0.484 |
| Dosages (g/L) × Slow mixing time (min) | -0.2593 | 0.484 |
| pH × [Lignin] (ppm) | -0.0105 | 0.831 |
| pH × Slow mixing time (min) | 0.0036 | 0.976 |
| [Lignin] (ppm) × Slow mixing time (min) | 0.0072 | 0.338 |

*3.2.2 Effect of independent variables on lignin removal efficiency (Y)*

The effect of the four parameters as Fe-BTC dosage, pH, initial lignin concentration, and slow mixing time on percentage of lignin removal is shown in Figure 3. Figure 3(a) shows that lignin removal efficiency decreased dramatically with Fe-BTC dosage from 1 to 2 g/L and then decreased gradually with 3 g/L. Lignin removal efficiency increased slightly from 50 to 100 ppm initial lignin concentration and then sharply increased to 150 ppm. Impact of slow mixing time to removal

**Table 4.** Experimental design matrix and lignin removal from the experimental data compared to the predicted values obtained from BBD

| Run No. | $X_1$ (g/L) | $X_2$ | $X_3$ (ppm) | $X_4$ (min) | Removal efficiency (%) | |
|---|---|---|---|---|---|---|
| | | | | | Lignin | |
| | | | | | Experimental | Predicted |
| 1 | 3 | 7 | 100 | 0 | 56.04 | 54.95 |
| 2 | 2 | 4 | 100 | 40 | 79.42 | 66.33 |
| 3 | 2 | 10 | 100 | 0 | 46.13 | 53.44 |
| 4 | 2 | 7 | 100 | 20 | 71.94 | 68.64 |
| 5 | 1 | 7 | 150 | 20 | 85.37 | 100.93 |
| 6 | 3 | 4 | 100 | 20 | 55.50 | 68.99 |
| 7 | 2 | 7 | 50 | 40 | 27.75 | 53.16 |
| 8 | 2 | 7 | 150 | 40 | 83.69 | 85.70 |
| 9 | 1 | 7 | 100 | 0 | 64.65 | 60.13 |
| 10 | 3 | 7 | 150 | 20 | 78.43 | 75.01 |
| 11 | 1 | 7 | 100 | 40 | 87.08 | 82.28 |
| 12 | 1 | 4 | 100 | 20 | 85.04 | 82.99 |
| 13 | 2 | 7 | 150 | 0 | 73.32 | 59.57 |
| 14 | 3 | 10 | 100 | 20 | 52.62 | 66.33 |
| 15 | 2 | 10 | 150 | 20 | 85.27 | 82.51 |
| 16 | 2 | 10 | 100 | 40 | 73.84 | 65.66 |
| 17 | 3 | 7 | 50 | 20 | 88.53 | 67.19 |
| 18 | 2 | 7 | 100 | 20 | 66.84 | 68.64 |
| 19 | 2 | 4 | 150 | 20 | 84.39 | 86.76 |
| 20 | 2 | 4 | 50 | 20 | 68.56 | 65.43 |
| 21 | 1 | 10 | 100 | 20 | 85.27 | 83.43 |
| 22 | 1 | 7 | 50 | 20 | 74.72 | 72.36 |
| 23 | 2 | 4 | 100 | 0 | 52.59 | 54.98 |
| 24 | 2 | 10 | 50 | 20 | 75.71 | 67.46 |
| 25 | 2 | 7 | 50 | 0 | 46.06 | 55.72 |
| 26 | 2 | 7 | 100 | 20 | 67.13 | 68.64 |
| 27 | 3 | 7 | 100 | 40 | 57.72 | 56.36 |
| | | | S.D. (%) | | 21.80 | |

efficiency increased from 0 to 20 min and then reduced between 20 and 40 min. Results revealed that the floc was broken down in the long-term due to the force of mixing (Zhang et al., 2013; Jiang, 2015). Meanwhile, effect of pH wastewater values was not significant. Percentage of lignin removal decreased considerably as the Fe-BTC dosage decreased. By contrast, percentage of lignin removal increased as initial lignin concentration increased. The contour plot in Figure 3b reveals that maximum lignin removal was greater than 80% at the optimal condition of Fe-BTC dosage at 2.0-3.0 g/L, pH 4.0-5.0 and 9.0-10.0, initial lignin concentration of 50-75 and 125-150 ppm, and slow mixing time of 15-25 and 35-40 min.

*3.2.3 Equation fitting model test*

Two runs of additional experiments were tested to confirm the equation fitting model. Table 5 depicts removal efficiency of lignin as a function of the chosen conditions for dosage of Fe-BTC, initial pH, initial lignin concentration, and slow mixing time. These two trials gave results close to the estimation, proving fitting model reliability.

(a)

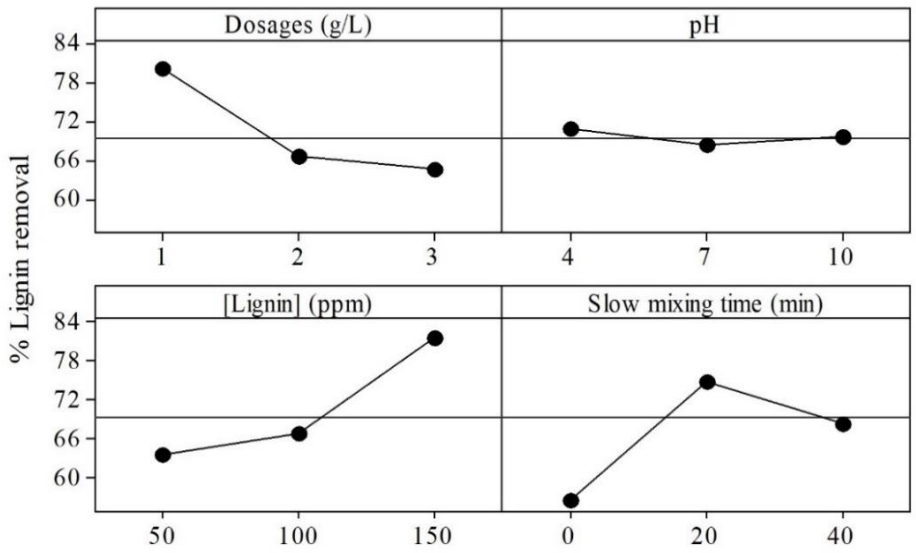


(b)

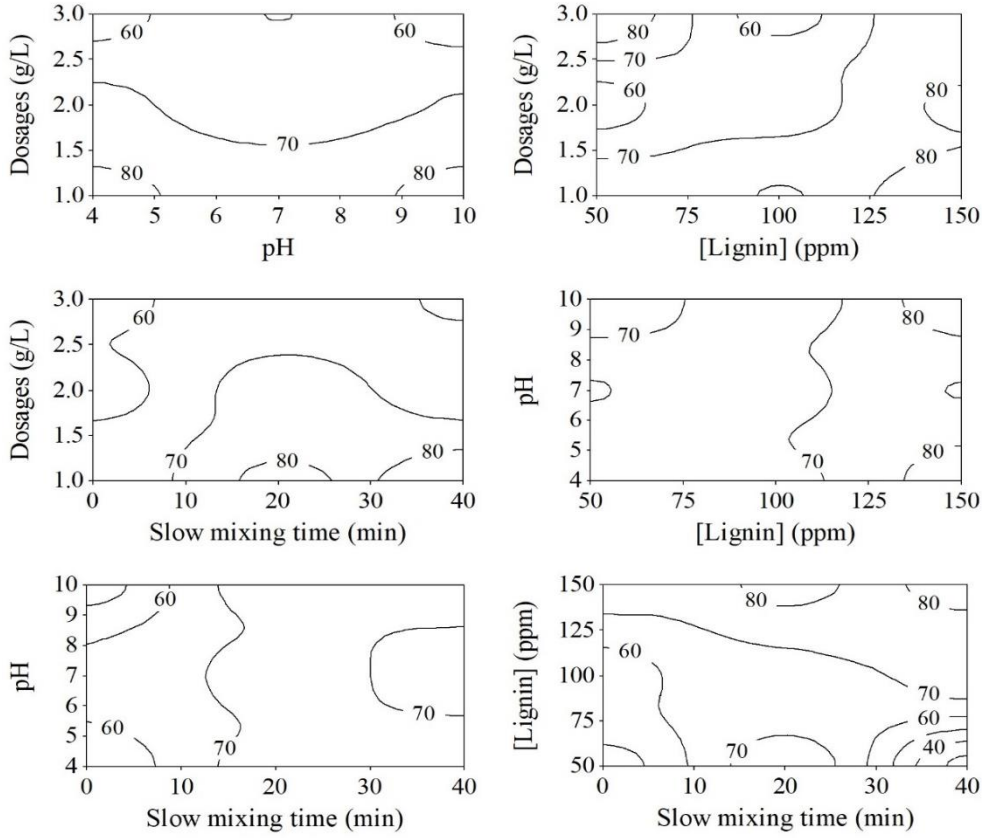


**Figure 3.** Variable effect on lignin removal efficiency (%) by Fe-BTC in uncoded value: (a) main effect plot and (b) contour plot.

**Table 5.** Confirmation experiments

| Conditions | $X_1$ (g/L) | $X_2$ | $X_3$ (ppm) | $X_4$ (min) | Removal efficiency (%) | |
|---|---|---|---|---|---|---|
| | | | | | Lignin | |
| | | | | | Experimental | Predicted |
| 1 | 2 | 6 | 150 | 30 | 70.76 | 87.73 |
| 2 | 3 | 8 | 100 | 10 | 63.18 | 62.72 |

Coagulation-flocculation test results indicated that Fe-BTC usage to remove lignin revealed three layers as Fe-BTC powder at the bottom, lignin sludge in the middle, and clear supernatant at the top because of its high stability and biocompatibility (Dhakshinamoorthy et al., 2012; Zhu et al., 2012). Furthermore, pH of treated samples was below 3 in all experiments performed since Fe-BTC has Lewis-acid catalyst properties (Majano et al., 2013).

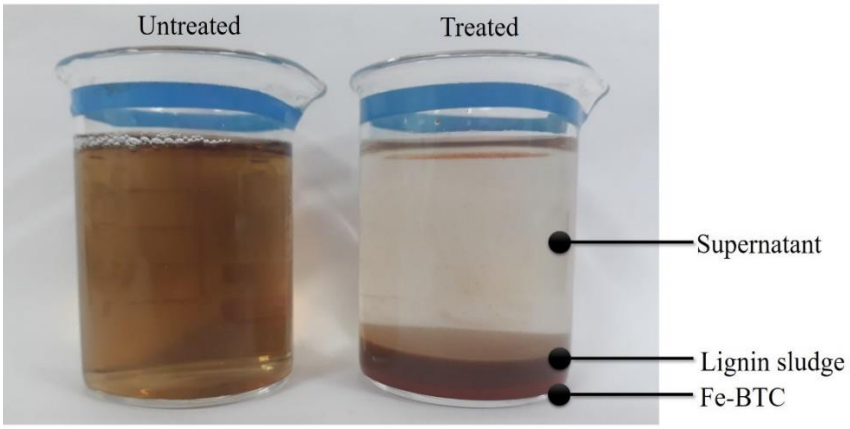


**Figure 4.** Wastewater separation into three layers: Fe-BTC powder at the bottom, lignin sludge in the middle and clear supernatant at the top.

Therefore, adsorption-charge neutralization mechanisms could play a major role (Zhang et al., 2017). Moreover, lignin sludge can be separated and recycled as a bio-adsorbent (Ge and Li, 2018), natural bio-polymer (Roopan, 2017), and component in plastics (Kun and Pukánszky, 2017).

## 4. CONCLUSIONS

BBD can optimize conditions of lignin removal using Fe-BTC as a coagulant to treat P&P effluent wastewater. Results suggested that Fe-BTC can be used as an alternative coagulant-flocculant to separate lignin from P&P effluent wastewater. Four influential parameters as Fe-BTC dosage (g/L), pH, initial lignin concentration (ppm) and slow mixing time (time) were tested. Findings revealed that the most influential factor affecting lignin removal was initial lignin concentration (p-values>0.05). To confirm the equation fitting model, two runs of additional experiments were operated. Results confirmed the data predicted by the model. These experiments demonstrated that the developed models were reliable. Additionally, the pH of treated samples was below 3 in all experiments performed, therefore, adsorption-charge neutralization mechanisms could play a major role.

The principle of coagulation-flocculation generally involves rapid mixing using coagulants to destabilize the colloids and slow mixing using flocculants to aggregate small particles into large flocs in the sedimentation tank. Using Fe-BTC as a coagulant aid could combine these steps into one mixing process and reduce chemicals, time, cost and ease of operation. Moreover, lignin sludge can be separated and recycled as a bio-adsorbent, natural bio-polymer, and component in plastics. Future research is required to investigate more effective pilot-scale testing to treat effluents resulting from P&P industrial wastewater. Sludge recycling studies are also necessary to improve ecological disposal methods for commercial material (Basolite® F300).

## ACKNOWLEDGEMENTS

This work was supported by the Office of Higher Education Commission (OHEC), the S&T Postgraduate Education and Research Development Office (PERDO), the Advanced Functional nanomaterials and Membrane for Environmental Remediation (AFMER) Research Unit, the Center of Excellence on Hazardous Substance Management (HSM), Chulalongkorn University, and Khon Kaen University's Graduate Research Fund, Academic Year 2016.

## REFERENCES


Ali M, Sreekrishnan TR. Aquatic toxicity from pulp and paper mill effluents: A review. Advances in Environmental Research 2001;5(2):175-96.

Andersson KI, Eriksson M, Norgren M. Removal of lignin from wastewater generated by mechanical pulping using activated charcoal and fly ash: Adsorption isotherms and thermodynamics. Industrial and Engineering Chemistry Research 2011;50(13):7722-32.

Aqil M, Kamran M, Ahad A, Imam SS. Development of clove oil based nanoemulsion of olmesartan for transdermal delivery: Box-Behnken design optimization and pharmacokinetic evaluation. Journal of Molecular Liquids 2016;214:238-48.

Archariyapanyakul P, Pangkumhang B, Khamdahsag P, Tanboonchuy V. Synthesis of silica-supported nanoiron for Cr(VI) removal: Application of Box-Behnken statistical design (BBD). Sains Malaysiana 2017;46(4):655-65.

Ashrafi O, Yerushalmi L, Haghighat F. Wastewater treatment in the pulp-and-paper industry: A review of treatment processes and the associated greenhouse gas emission. Journal of Environmental Management 2015;158:146-57.

Autie-Castro G, Autie MA, Rodríguez-Castellón E, Aguirre C, Reguera E. Cu-BTC and Fe-BTC metal-organic frameworks: Role of the materials structural features on their performance for volatile hydrocarbons separation. Colloids and Surfaces A: Physicochemical and Engineering Aspects 2015;481:351-7.

Bezerra MA, Santelli RE, Oliveira EP, Villar LS, Escaleira LA. Response surface methodology (RSM) as a tool for optimization in analytical chemistry. Talanta 2008;76(5):965-77.

Bilici Baskan M, Pala A. A statistical experiment design approach for arsenic removal by coagulation process using aluminum sulfate. Desalination 2010;254(1-3): 42-8.

Daud NM, Sheikh Abdullah SR, Abu Hasan H. Response surface methodological analysis for the optimization of acid-catalyzed transesterification biodiesel wastewater pre-treatment using coagulation-flocculation process. Process Safety and Environmental Protection 2018;113:184-92.

Dhakshinamoorthy A, Alvaro M, Chevreau H, Horcajada P, Devic T, Serre C, Garcia H. Iron(III) metal-organic frameworks as solid Lewis acids for the isomerization of α-pinene oxide. Catalysis Science and Technology 2012;2(2):324-30.

Duan J, Gregory J. Coagulation by hydrolysing metal salts. Advances in Colloid and Interface Science 2003;100-102:475-502.

Ferreira SLC, Bruns RE, Ferreira HS, Matos GD, David JM, Brandão GC. Box-Behnken design: An alternative for the optimization of analytical methods. Analytica Chimica Acta 2007;597(2):179-86.

Folens K, Huysman S, Van Hulle S, Du Laing G. Chemical and economic optimization of the coagulation-flocculation process for silver removal and recovery from industrial wastewater. Separation and Purification Technology 2017;179:145-51.

Ge Y, Li Z. Application of lignin and its derivatives in adsorption of heavy metal ions in water: A Review. ACS Sustainable Chemistry and Engineering 2018; 6(5):7181-92.

Haq I, Kumar S, Raj A, Lohani M, Satyanarayana GNV. Genotoxicity assessment of pulp and paper mill effluent before and after bacterial degradation using Allium cepa test. Chemosphere 2017;169:642-50.

Hu X, Lou X, Li C, Ning Y, Liao Y, Chen Q, Mananga ES, Shen M, Hu B. Facile synthesis of the Basolite F300-like nanoscale Fe-BTC framework and its lithium storage properties. RSC Advances 2016; 6(115):114483-90.

Huang S, Yang K, Liu X, Pan H, Zhang H, Yang S. MIL-100(Fe)-catalyzed efficient conversion of hexoses to lactic acid. RSC Advances 2017;7:5621-7.

Jiang JQ. The role of coagulation in water treatment. Chemical Engineering 2015;8:36-44.

Kamali M, Khodaparast Z. Review on recent developments on pulp and paper mill wastewater treatment. Ecotoxicology and Environmental Safety 2015;114:326-42.

Khamdahsag P, Thongkao W, Saowapakpongchai A, Tanboonchuy V. Kaolin Modified Nano Zero Valent Iron Synthesis via Box-Behnken Design Optimization. Applied Environmental Research 2017;39(2):55-65.

Kiattisaksiri P, Khamdahsag P, Khemthong P, Pimpha N, Grisdanurak N. Photocatalytic degradation of 2,4-dichlorophenol over Fe-ZnO catalyst under visible light. Korean Journal of Chemical Engineering 2015;32:1578-85.

Kim SC. Application of response surface method as an experimental design to optimize coagulation-flocculation process for pre-treating paper wastewater. Journal of Industrial and Engineering Chemistry 2016;38:93-102.

Kun D, Pukánszky B. Polymer/lignin blends: Interactions, properties, applications. European Polymer Journal 2017;93:618-41.

Lee CS, Robinson J, Chong MF. A review on application of flocculants in wastewater treatment. Process Safety and Environmental Protection 2014;92(6):489-508.

Lee KE, Morad N, Teng TT, Poh BT. Development, characterization and the application of hybrid materials in coagulation/flocculation of wastewater: A review. Chemical Engineering Journal 2012;203:370-86.

Li X, Guo W, Liu Z, Wang R, Liu H. Fe-based MOFs for

efficient adsorption and degradation of acid orange 7 in aqueous solution via persulfate activation. Applied Surface Science 2016;369:130-6.

Lindholm-Lehto PC, Knuutinen JS, Ahkola HSJ, Herve SH. Refractory organic pollutants and toxicity in pulp and paper mill wastewaters. Environmental Science and Pollution Research 2015;22(9):6473-99.

Luekittisup P, Tanboonchauy V, Chumee J, Predapitakkun S, Kiatkomol RW, Grisdanurak N. Removal of chlorinated chemicals in $H_2$ feedstock using modified activated carbon. Journal of Chemistry 2015;2015:1-9.

Mahmoodi NM, Abdi J, Oveisi M, Alinia Asli M, Vossoughi M. Metal-organic framework (MIL-100 (Fe)): Synthesis, detailed photocatalytic dye degradation ability in colored textile wastewater and recycling. Materials Research Bulletin 2018;100:357-66.

Majano G, Ingold O, Yulikov M, Jeschke G, Pérez-Ramírez J. Room-temperature synthesis of Fe-BTC from layered iron hydroxides: The influence of precursor organisation. CrystEngComm 2013;15(46): 9885-93.

Naseem A, Tabasum S, Zia KM, Zuber M, Ali M, Noreen A. Lignin-derivatives based polymers, blends and composites: A review. International Journal of Biological Macromolecules 2016;93:296-313.

Phanthasri J, Khamdahsag P, Jutaporn P, Sorachoti K, Wantala K, Tanboonchuy V. Enhancement of arsenite removal using manganese oxide coupled with iron (III) trimesic. Applied Surface Science 2018;427:545-52.

Renault F, Sancey B, Badot PM, Crini G. Chitosan for coagulation/flocculation processes - An eco-friendly approach. European Polymer Journal 2009;45(5): 1337-48.

Roopan SM. An overview of natural renewable bio-polymer lignin towards nano and biotechnological applications. International Journal of Biological Macromolecules 2017;103:508-14.

Sillanpää M, Ncibi MC, Matilainen A, Vepsäläinen M. Removal of natural organic matter in drinking water treatment by coagulation: A comprehensive review. Chemosphere 2018;190:54-71.

Sun Y, Zhu C, Zheng H, Sun W, Xu Y, Xiao X, You Z, Liu C. Characterization and coagulation behavior of polymeric aluminum ferric silicate for high-concentration oily wastewater treatment. Chemical Engineering Research and Design 2017;119:23-32.

Tak Bong-yul, Tak Bong-sik, Kim Young-ju, Park Yong-jin, Yoon Young-hun, Min Gil-ho. Optimization of color and COD removal from livestock wastewater by electrocoagulation process: Application of Box-Behnken design (BBD). Journal of Industrial and Engineering Chemistry 2015;28:307-15.

Yang Y, Bai Y, Zhao F, Yao E, Yi J, Xuan C, Chen S. Effects of metal organic framework Fe-BTC on the thermal decomposition of ammonium perchlorate. RSC Advances. 2016;6(71):67308-14.

Zahrim AY, Nasimah A, Hilal N. Coagulation/flocculation of lignin aqueous solution in single stage mixing tank system: Modeling and optimization by response surface methodology. Journal of Environmental Chemical Engineering 2015;3(3):2145-54.

Zhan X, Gao B, Yue Q, Wang Y, Cao B. Coagulation behavior of polyferric chloride for removing NOM from surface water with low concentration of organic matter and its effect on chlorine decay model. Separation and Purification Technology 2010;75(1):61-8.

Zhang Z, Liu D, Hu D, Li D, Ren X, Cheng Y, Luan Z. Effects of slow-mixing on the coagulation performance of polyaluminum chloride (PACI). Chinese Journal of Chemical Engineering 2013;21(3):318-23.

Zhang Z, Wang J, Liu D, Li J, Wang X, Song B, Yue B, Zhao K, Song Y. Hydrolysis of polyaluminum chloride prior to coagulation: Effects on coagulation behavior and implications for improving coagulation performance. Journal of Environmental Sciences 2017;57:162-9.

Zhu B, Yu X, Jia Y, Peng F, Sun B, Zhang M, Luo T, Liu J, Huang X. Iron and 1,3,5-benzenetricarboxylic metal-organic coordination polymers prepared by solvothermal method and their application in efficient As(V) removal from aqueous solutions. The Journal of Physical Chemistry C 2012;116(5):8601-7.